land

MDPI

Article

A New GIS-Based Framework to Detect Urban Heat Islands and Its Application on the City of Naples (Italy)

Rosa Cafaro [1], Barbara Cardone [1], Valeria D'Ambrosio [1], Ferdinando Di Martino [1,2,*] and Vittorio Miraglia [1]

[1] Department of Architecture, University of Naples Federico II, Via Toledo 402, 80134 Napoli, Italy; rosa.cafaro@unina.it (R.C.); b.cardone@unina.it (B.C.); valeria.dambrosio@unina.it (V.D.); vittorio.miraglia@unina.it (V.M.)

[2] Center for Interdepartmental Research "Alberto Calza Bini", University of Naples Federico II, Via Toledo 402, 80134 Napoli, Italy

* Correspondence: fdimarti@unina.it; Tel.: +39-081-2538904

Abstract: This research presents a GIS-based framework used to detect urban heat islands and determine which urban settlement elements are most critical when heatwave risks exist. The proposed method uses the Iterative Self-Organizing Data Analysis (ISODATA) clustering algorithm applied to the satellite land surface temperature distribution recorded during heatwaves for the detection of urban heat islands. A pixel classification confidence level maximization approach, obtained by running a maximum likelihood classification algorithm, is performed to determine the optimal number of clusters. The areas labeled as hotspots constitute the detected urban heat islands (UHIs). This method was tested on an urban settlement set up by the municipality of Naples (Italy). Comparison tests were performed with other urban heat island detection methods such as standard deviation thresholding and Getis-Ord Gi* hotspot detection; indices measuring the density of buildings, the percentage of permeable open spaces, and vegetation cover are taken into consideration to evaluate the accuracy of the urban heat islands detected. These tests highlight that the proposed method provides the most accurate results. It could be an effective tool to support the decision maker in evaluating which urban areas are the most critical during heatwave scenarios.

Keywords: UHI; UHI detection; heatwave; LST; GIS; ISODATA; maximum likelihood classification

Citation: Cafaro, R.; Cardone, B.; D'Ambrosio, V.; Di Martino, F.; Miraglia, V. A New GIS-Based Framework to Detect Urban Heat Islands and Its Application on the City of Naples (Italy). *Land* **2024**, *13*, 1253. https://doi.org/10.3390/land13081253

Academic Editor: Guoyu Ren

Received: 26 July 2024
Revised: 1 August 2024
Accepted: 8 August 2024
Published: 9 August 2024

1. Introduction

Urban heat islands (UHIs) are one of the most significant and well-documented phenomena of human-induced climate change [1–3], initially described by Oke in [4]. UHIs refer to cities experiencing higher temperatures than their surrounding non-built areas, primarily due to landscape modifications, high densities of impervious surfaces, and a lower expanse of green vegetated areas [5].

Climate projections indicate that the intensity and frequency of heatwaves will increase significantly in the coming decades, exacerbating the effects of UHIs in urban areas [6]. This scenario further accentuates the need to develop accurate tools for the detection and mitigation of UHIs, as cities will face increasingly intense thermal challenges that could compromise urban livability and public health [7].

In the context of increasing climate vulnerability, the role of urban planners becomes fundamental. Accurately detecting and analyzing UHIs is essential for developing effective mitigation strategies [8].

Historically, most UHI detection studies were limited to using few fixed weather stations, low-spatiotemporal-resolution satellite imagery, or small-scale mobile measurements made with automobiles. These limitations prevented the detailed detection of thermal variations within urban areas [9].

At present, thanks to technological advances, and particularly the improved spatiotemporal resolution of satellite images, it has become possible to analyze temperature differences within a city with greater accuracy.

In this context, the land surface temperature (LST) index, detected using remote sensing techniques, has emerged as a key tool for the accurate assessment of urban climate and heat islands. Compared to traditional methods, the LST index offers broader and more detailed spatial coverage, allowing for a more accurate and complete analysis of thermal variations in urban areas [10,11].

While LST data from satellite imagery have greatly improved our ability to study UHIs, existing UHI detection methods still have significant limitations [12]. Two commonly used approaches are the Getis-Ord Gi* hotspot detection algorithm [13] and the standard deviation-based [14] UHI detection method. However, these techniques often fall short in providing reliable and consistent UHI identification.

The Getis-Ord Gi* statistic, while useful for identifying spatial clusters of high or low values, is highly sensitive to the choice of spatial weights and the size of the study area. This can lead to inconsistent results, where UHIs are identified differently depending on the specific parameterization used [12].

Standard deviation methods, which classify areas as heat islands based on their deviation from the mean temperature, also have drawbacks. They assume a normal distribution of temperatures and can be overly influenced by extreme values, potentially misidentifying UHIs in areas with high temperature variability [13,14].

Both these methods share a common limitation: they often produce unstable hotspots, where areas are identified as critical only under specific parameter combinations. This instability can lead to unreliable results and, consequently, to misguided urban planning decisions. An urban planner relying on such information may incorrectly prioritize areas for intervention, potentially misallocating a city's limited resources.

Given the increasing importance of accurate UHI detection, there is a clear need for more robust and reliable methods.

To address these challenges, this study presents an unsupervised UHI detection method based on a clustering algorithm, called Iterative Self-Organizing Data Analysis (ISODATA), for processing LST data during a heatwave in an urban settlement, with the objective of identifying temperature clusters associated with urban heat islands. The proposed approach allows us to automatically obtain temperature clusters representative of an UHI, avoiding the need to predefine the number of clusters, as is required by techniques commonly used in the literature, such as K-means and Fuzzy C-means. These traditional techniques, widely employed in UHI analysis, require the user to specify the number of clusters a priori, which can significantly influence the results and often requires in-depth knowledge of the study area or a process of iterative optimization; furthermore, these algorithms are not very robust to the presence of noise and outliers in the data.

In the proposed method, a fast iterative process is used to set the optimal number of clusters; in addition, the use of the ISODATA algorithm has the advantage of discarding incorrect clusters generated due to noise or outliers.

The performance of this proposed method is analyzed and compared with other well-known methods widely used for UHI detection, such as Getis-Ord Gi* hotspot analysis and standard deviation thresholding, to evaluate which approach provides a more accurate and detailed representation of the thermal characteristics of urban soil. In particular, in order to evaluate the accuracy of the three UHI detection methods, three typical characteristics of an urban settlement are analyzed in each UHI—the volume of buildings, the permeability of soils, and the extent of green areas—to analyze how they are different in the UHIs compared to the entire urban study area. The tests carried out on the city of Naples, in Italy, show that the proposed method is the most accurate as it manages to label as UHIs the areas of the city with a higher building density and soil permeability and with the lowest concentration of vegetated areas.

The proposed method was implemented on a GIS platform; this is a powerful tool for urban planners and policy makers, enabling more informed urban planning aimed at mitigating heat island effects.

The State of the Art

The evolution of remote sensing techniques and geospatial tools has revolutionized the study of urban heat islands, opening new frontiers in the analysis of this crucial phenomenon. These technological advancements offer large dataset processing capabilities and sophisticated spatial analysis, overcoming the limitations of traditional methods based on in situ measurements. While air temperature data from observatories are often limited by the number of stations available, restricting the analysis both temporally and spatially, remote sensing allows larger areas to be captured with extended temporal coverage. Furthermore, integrating remote sensing data with advanced geospatial tools enables more detailed and complex spatial analyses, facilitating the understanding of large-scale urban thermal patterns. This methodological transition has led to the development of a variety of analytical approaches, from the analysis of temperature differences between urban and rural areas to advanced spatial clustering techniques, reflecting the complexity and dynamicity of the UHI phenomenon.

Starting from simple comparative approaches, research has moved towards increasingly sophisticated spatial analysis and clustering techniques. A widely used approach to quantify urban heat island intensity is the urban–rural difference method. This method compares the average LST of urban areas with that of surrounding rural areas [15]. However, this approach has some limitations, particularly in the context of rapid and persistent urbanization. With the continuous expansion of urban areas and the progressive transformation of peri-urban areas, it becomes increasingly difficult to clearly delineate the boundary between urban and rural areas. This ambiguity in the definition of these limits can significantly influence the results of the analysis, making the quantification of the intensity and extent of UHIs based exclusively on the urban–rural comparison less reliable [16,17].

Another method consists of dividing the LST into multiple temperature groups (e.g., high, medium–high, medium, medium–low, low) based on a threshold method, and then identifying the spatial extent of the group with the highest temperature as the UHI region [18,19]. This approach has some significant limitations. First, its methodology may be overly simplified and prone to errors, as it does not adequately take into account the different factors that influence LST and the specific characteristics of urban environments. Furthermore, a critical aspect is that the results of UHI identification can vary significantly depending on the thresholding algorithm used. The main threshold algorithms used are Fixed Thresholds and the standard deviation method.

Hotspot analysis, particularly using the Getis-Ord Gi* statistic, represents a significant advancement in the detection and analysis of urban heat islands (UHIa). This method is notable for its ability to identify statistically significant clusters of elevated temperatures, offering a more robust and objective basis for delineating UHIs than previous methods. The Getis-Ord Gi* statistic examines each feature (each temperature pixel) in the context of its neighboring features and calculates the sum of the value of a feature and its neighbors, comparing it proportionally to the sum of all features. When the local sum is significantly different from the expected one, and this difference is too large to be the result of chance, a statistically significant z-score is obtained.

This method has the advantage of identifying high-temperature clusters that are statistically significant, reducing the influence of random fluctuations; evaluating each point in relation to its surroundings, better capturing the spatially continuous nature of UHIs; and detecting hotspots at different spatial scales, adapting to the variability of an urban structure. Several studies have successfully applied a Getis-Ord Gi* analysis to study UHIs.

In [20], Cheval and Dumitrescu used this technique to identify significant thermal hotspots, revealing a concentration of "very hotspots" in the city center of Bucharest and

along its main traffic arteries. The Getis-Ord Gi* was applied to a study of the metropolitan area of Florence in Tuscany (Italy) [21]. This technique was used to map and evaluate daytime summer thermal hotspots and cold spots in relation to the characteristics of urban greenery, urban surfaces, and city morphology. The analysis was based on land surface temperature (LST) data obtained from the Landsat 8 satellite during summer daytime periods from 2015 to 2019. By applying the Getis-Ord Gi* to average summer LST datasets, the study allowed us to identify the location and boundaries of hotspots and cold spots. However, this method may have limitations that depend on the quality and resolution of the input data, which can strongly influence the accuracy of the analysis.

Some other studies have investigated the phenomenon of UHIs through the use of spatial unsupervised clustering techniques, such as K-means, to group areas with similar thermal characteristics. These clustering methods are particularly effective for processing satellite images without prior knowledge, as they group pixels based on spectral variance. In [22], K-means clustering was used on Landsat 8 thermal data to map urban heat islands and correlate them with land use in the Turin metropolitan area. Luo et al., in [23], proposed a K-means clustering approach to analyze UHI intensity using temperature data. In another more recent study [24], the K-means clustering method was used to investigate the relationship between LST, building density (BD), and building height (BH) in urban environments. A fast variation of Fuzzy C-means is applied in [25] to segment remote-sensed images; the authors show that this method produces more accurate results than K-means and allows us to consider the spatial relationships between neighboring pixels. However, it too is not very robust with respect to the presence of noise and outliers in the image.

Furthermore, K-means and Fuzzy C-means clustering methods have the limitation of needing to fix the number of clusters a priori. To overcome this limitation, in our study we propose a UHI detection algorithm based on ISODATA, which has the advantages of automatically obtaining the optimal number temperature clusters representative of the UHI, avoiding the need to predefine the number of clusters, and is more robust to noise than K-means. ISODATA extracts the training samples automatically, setting them by dragging a window over the image. Numerous studies have successfully applied ISODATA to map and categorize different land cover types, taking advantage of its ability to identify natural clusters in multispectral data without the need for predefined training samples. It was utilized in [26] for land cover classification using Landsat 5 TM data. It successfully classified eight land cover classes with a 93% agreement with the reference map. ISODATA's classification accuracy is attributed to the behavior of means and standard deviations in the decision space. In [27], the authors use K-means and ISODATA clustering algorithms to map Local Climate Zones in the urban areas of Dhaka and Kolkata, finding that ISODATA is better at distinguishing between open and compact mid-rise urban types.

Despite its success in land use classification, the application of the ISODATA algorithm specifically for UHI detection remains a relatively unexplored field. Our study aims to fill this research gap by proposing a UHI detection method based on ISODATA. We compare its accuracy to that obtained using traditional UHI detection methods.

2. Methodology

2.1. The Proposed UHI Detection Method

Our UHI detection method executes an iterative process in which the ISODATA image clustering algorithm is applied to LST raster data.

Recent studies have used both the LST and the 2 m air temperature to investigate the behavior of urban atmospheric thermal environments during periods of extreme weather events such as heatwaves [28] and rainstorms [29]. They have highlighted that both the LST and the air temperatures are influenced by various climatic and urban soil characteristics; they can be useful in analyzing the mutual interactions between UHI, weather, and climate.

In [30], LST is used to analyze the effects of UHIs on heavy rainfall events. The results of tests performed on the coastal city of Nantong, near Shanghai, China, have shown

how the spatial information of surface temperature extracted from satellite observations allows us to analyze the complexity of the spatial variations of urban soil, which cannot be captured by atmospheric temperature measurements recorded by meteorological stations.

The use of the LST raster as input information for UHIs' detection is motivated by the fact that, unlike the air temperature measured by weather stations, LST can describe the variation in the type of soil and in its use, as well as the distribution of the type of urban settlement, representing a more significant parameter than the air temperature for the evaluation of the thermal response of urban soils.

ISODATA is a clustering algorithm applied to multivariate data given by one or more image bands. In our method, the ISODATA algorithm is executed only on LST raster data. The resulting signature file can be used as the input for a classification tool, such as maximum likelihood classification, that produces an unsupervised classification raster.

ISODATA uses a sample of data points assigned by considering a square window on the image of size $n_w \times n_w$ pixels and selecting the values of the central pixel of the window imposed on the image. The parameter n_w is called the *sampling interval*; it must be set to create the sample data. This approach has the advantage of reducing the size of the image dataset; however, an incorrect choice of sampling interval can generate insufficient sample data and provide inaccurate results.

To avoid under-sampling, the sampling interval is determined so that the size of the area covered by the window is approximately equal to 2% of the size of the area covered by the image.

For example, let us consider a satellite image given by 256 × 256 pixels, where the size of a pixel is 30 m × 30 m. The image covers an area of 1.97 km^2. Setting $n_w = 7$, we obtain a window of size 0.0441 km^2, equal to approximately 2% of the size of the area covered by the image. The sample dataset will be made up of 1338 pixels, which is approximately 2% of the number of pixels in the image.

Another parameter to be set is called the *Minimum class size*. This parameter represents the minimum number of pixels in the sample that can be assigned to a cluster; clusters consisting of fewer cells than the minimum class size will be eliminated at the end of the iterations.

A value of this parameter that is too low would affect clustering, as even very noisy pixels or outliers would be considered clusters. On the other hand, too high a value would lead to the removal of clusters that could be significant. To avoid these critical issues, a value of the minimum class size parameter equal to approximately 2% of the sample's cardinality is assigned. Considering the previous example, the value assigned to this parameter is 27 pixels, equal to approximately 2% of the number of pixels in the sample dataset.

Finally, as with K-means, in ISODATA it is necessary to assign the number C of clusters a priori. To set the optimal number of clusters, we analyze the confidence raster obtained by executing the maximum likelihood classification, for which every pixel is assigned the confidence level of its classification, where the confidence level is given by an integer value between 1 and 14, following the classification of the likelihood given in Table 1.

To determine the optimal number of clusters, the ISODATA algorithm is executed iteratively while varying the number of clusters from 2 to 10 each time. The optimal number of clusters C is given by the number of clusters for which the number of sample pixels with a confidence level between 9 and 14 (a likelihood probability less than 0.1) is at its minimum.

After obtaining the classification of the LST raster, those areas corresponding to contiguous pixels belonging to the class referred to by the cluster whose centroid has the highest average LST value are labeled as hotspots; vice versa, those areas corresponding to contiguous pixels belonging to the class referred to by the cluster whose centroid has the lowest average LST value are labeled as cold spots. The hotspots are extracted as polygons on the map; they represent a UHI in the urban area of study.

The flow diagram in Figure 1 schematizes the proposed UHI detection method.

Table 1. Confidence levels used in the maximum likelihood classification.

Likelihood Interval	Confidence Level
[0.995–1.000]	1
[0.990–0.995]	2
[0.975–0.990]	3
[0.950–0.975]	4
[0.900–0.950]	5
[0.750–0.900]	6
[0.500–0.750]	7
[0.250–0.500]	8
[0.100–0.250]	9
[0.050–0.100]	10
[0.025–0.050]	11
[0.010–0.025]	12
[0.005–0.010]	13
[0.000–0.005]	14

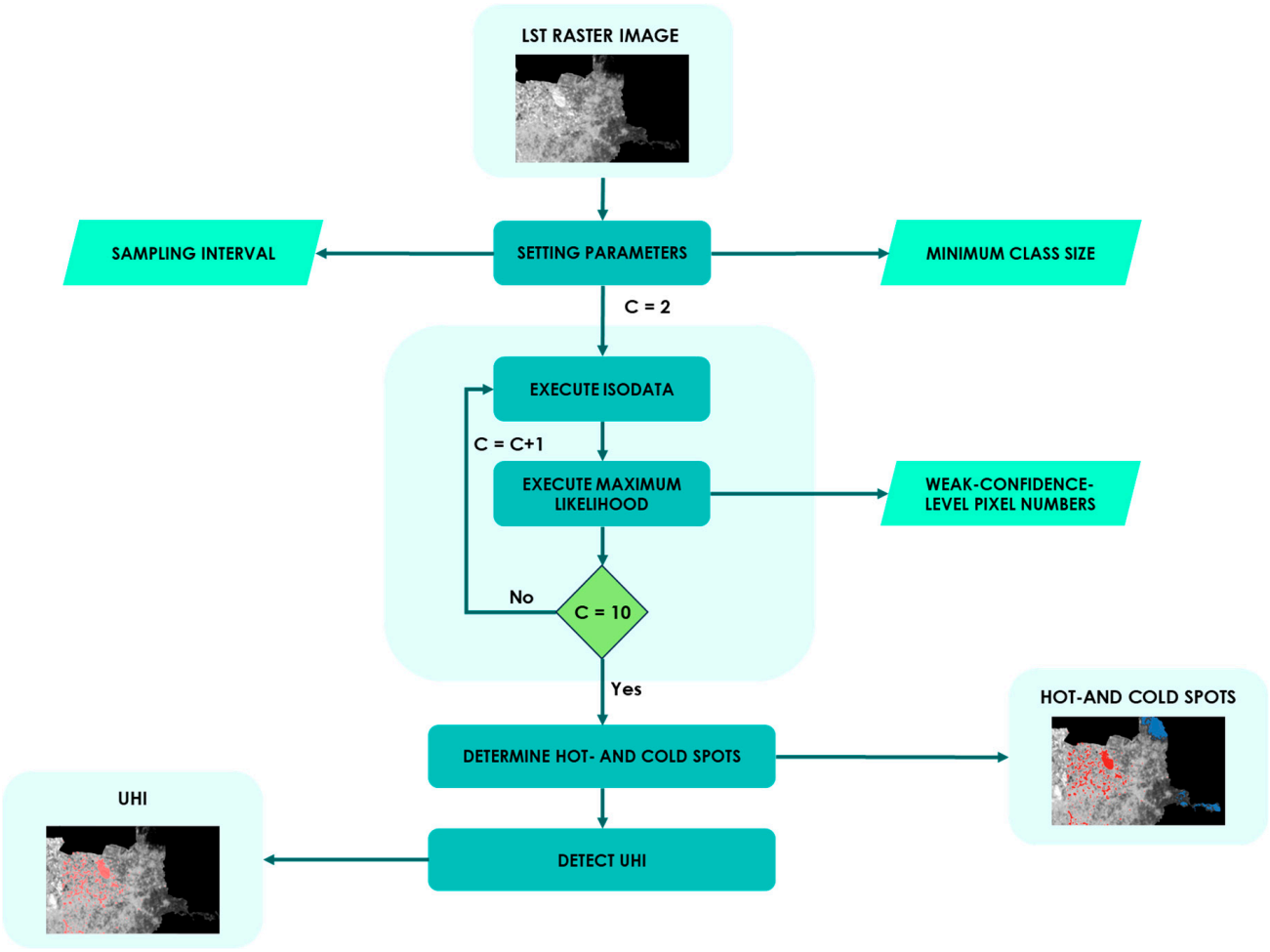

Figure 1. Flow diagram of the proposed method.

The *Setting Parameters* component fixes the value of the sampling interval n_w and of the minimum class size mcs, setting n_w to 2% of the size of the area covered by the image and mcs to 2% of the size of the sample. The minimum class size is given by 27 pixels.

The two components *Execute ISODATA* and *Execute Maximum Likelihood* are executed in sequence iteratively, varying the number of clusters from 2 to 10 and setting the optimal

number of clusters and the corresponding optimal classification as ones for which the number of sample pixels with a likelihood probability less than 0.1 is at its minimum.

The component *Determine Hot- and Cold Spots* marks hot- and cold spots. If μ_T and σ_T are the average and the standard deviation in the raster LST, all pixels belonging to classes with a mean LST greater than $\mu_T + \sigma_T$ are marked as hotspots; conversely, all pixels belonging to classes with a mean LST lower than $\mu_T - \sigma_T$ are marked as cold spots.

The component *Detect UHI* merges adjoint pixels labeled as hotspots, generating UHIs as polygons on the map. The characteristics of the UHIs can be analyzed by measuring the urban indices in the areas covered by them.

2.2. The Case Study: The City of Naples (Italy)

The urban area of study is the municipality of Naples, in Itay (Figure 2); it was selected as a case study as it is an urban settlement with a high mean population density and building density.

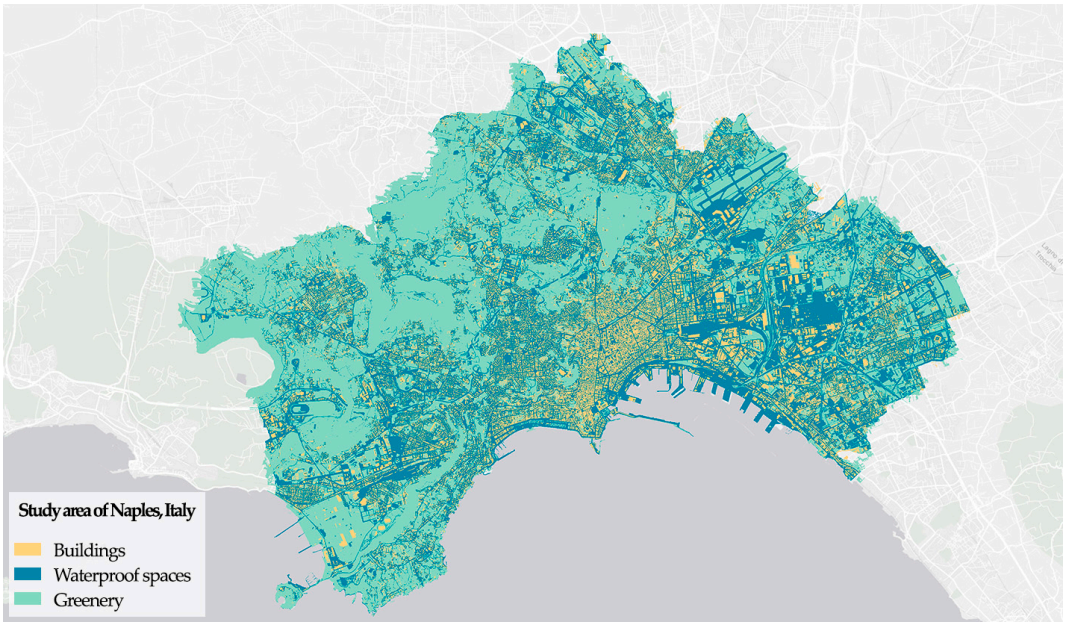

Figure 2. Study area of the city of Naples, Italy.

Naples is characterized by its modest expanse, equal to 11,727 hectares, and a very high population density, equal to 8566 inhabitants per square kilometer.

Despite the massive building expansion that occurred in the second half of the twentieth century, agricultural activities and natural areas are not absent from Naples.

In several areas of the historic and newly built city center, the growth of overbuilding and asphalted surfaces has intensified the risk of heat accumulations during the summer months, which have become increasingly intense in recent years due to the presence of heatwave scenarios that are lasting longer each time.

The historic city center is the area with the greatest population and built density; it is characterized by a high percentage of impervious open spaces and few urban green spaces. The western and northwestern outskirts of the city are characterized by a greater extension of forest-type green spaces than the rest of the city. The eastern suburbs are predominantly industrial, with a high density of buildings along the coast and a predominance of impervious open spaces.

In order to apply the proposed UHI detection method to this case study, the LST raster dataset of the city of Naples was extracted from the Landsat remotely sensed data, with a 30 × 30 m resolution, on 15 July 2023, during a heatwave period Figure 2. The raster LST is shown in Figure 3.

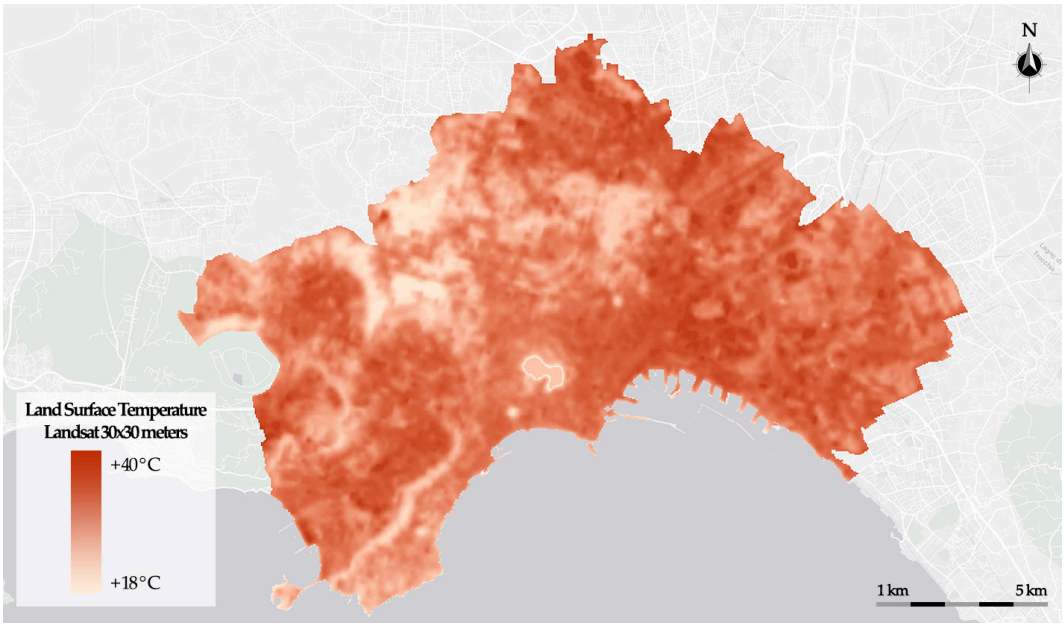

Figure 3. LST in the city of Naples, Italy, obtained on 15 July 2023.

LST varies in a range between 19.04 °C and 36.98 °C, where the average is μ_T = 28.10 °C and the standard deviation is σ_T = 2.67 °C.

The urban green areas are extracted as polygons from a regional topographic database at a 1:5000.

This method was implemented using the GIS platform ESRI ArcGIS Pro 3.3 and the ESRI ArcGIS Python library.

In the next section, the results obtained are presented and discussed and can vary significantly depending on the thresholding algorithm used. Each algorithm can establish different thresholds for classifying temperatures, leading to different interpretations of which areas are considered UHIs [23].

3. Results and Discussion

The proposed ISODATA UHI detection method was tested on the LST raster of the city of Naples, with a sampling interval set to n_w = 10 m, in order to obtain a corresponding window size n approximately equal to 2% of the size of the area covered by the raster LST. The sampling dataset is 1338 pixels. The minimum class size is set to 27 pixels, which is about 2% of the size of the sampling dataset.

The optimal number of clusters is seven. For each class in Table 2, the mean LST of the corresponding class and the labeling of the pixels belonging to that class are shown.

Table 2. Mean LST value of the seven classes and the labeling of the pixels.

Class ID	Mean LST (°C)	Pixel Labeling
1	22.35	Cold spot
2	24.66	Cold spot
3	26.49	-
4	27.94	-
5	29.15	-
6	30.34	-
7	31.60	Hotspot

Since $\mu_T - \sigma_T$ = 25.43 °C, all pixels belonging to the first two classes are marked as cold spots. Furthermore, since $\mu_T + \sigma_T$ = 30.77 °C, all pixels belonging to the last class are marked as hotspots.

In Figure 4 is shown a thematic map of the LST, classified by the seven classes. In the legend, each class is labeled with a mean land surface temperature.

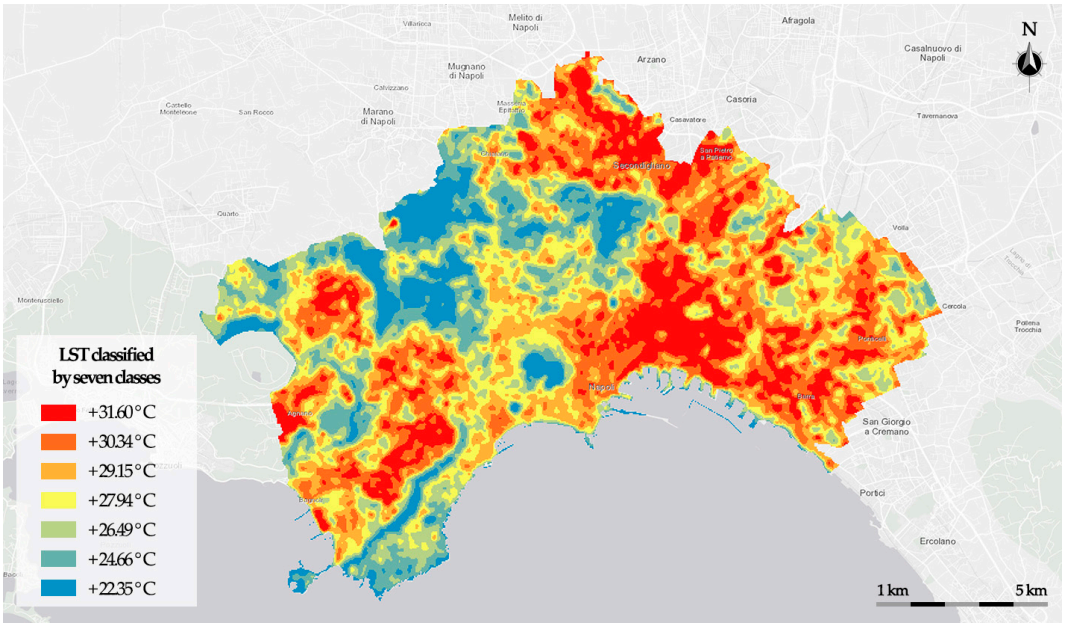

Figure 4. LST classification obtained with the proposed model.

Adjoined pixels belonging to the last class are merged to form hotspots; the hotspots constitute the UHIs detected in the city.

A comparison was performed with the standard deviation method and Getis-Ord Gi* UHI detection method.

The standard deviation method was executed by identifying the UHI patches as those areas that enclose contiguous pixels with LST values greater than the average LST value plus half the standard deviation.

The Getis-Ord G* method was executed by using the inverse distance method to assign to neighboring data points a larger influence than data points that are far away. Euclidean metrics was selected to calculate the distances between data points.

Figures 5–7 show, respectively, the UHI maps obtained using the standard deviation method, the Getis-Ord Gi* algorithm, and the proposed UHI detection method based on the ISODATA algorithm.

The map of the UHIs detected using the standard deviation method (Figure 5) shows a higher concentration of hotspots in the eastern central area of the city of Naples. This method also identifies large hotspots located in the western area, in the northern zone, and in the south-eastern districts. There are also some very small hotspots, mainly distributed in the central area of the study area.

Figure 6 shows the UHIs obtained by executing the Getis-Ord Gi* method; in it are present a low number of UHIs but with wide surface extensions. In line with the results of the standard deviation method, the south-eastern area is the most affected by the UHI phenomenon. In fact, there is a large hotspot that extends from the eastern districts to northern districts. Also, in this case, districts in the western area are affected by UHIs. There are also some small hotspots, mainly concentrated in the central area of the study area. With respect to the UHI map obtained by executing the standard deviation method, in this map are located a lower number of UHIs which have a greater extension.

The map of the UHIs detected by executing our proposed method is shown in Figure 7. It shows a larger number of UHIs with a smaller surface extension with respect to the UHIs detected by executing the other two methods. Comparing this map with the two previous ones, in line with the other distributions, a high concentration of UHIs in the south-eastern

zone is highlighted, while other UHIs are present in the northern zone and in the western zone; in contrast, the districts located in the center do not contain UHIs. The UHIs with the greatest extension are located in the central south-eastern area and cover most of these districts. Other large UHIs are found in the northern districts, in the western districts, and in the eastern districts.

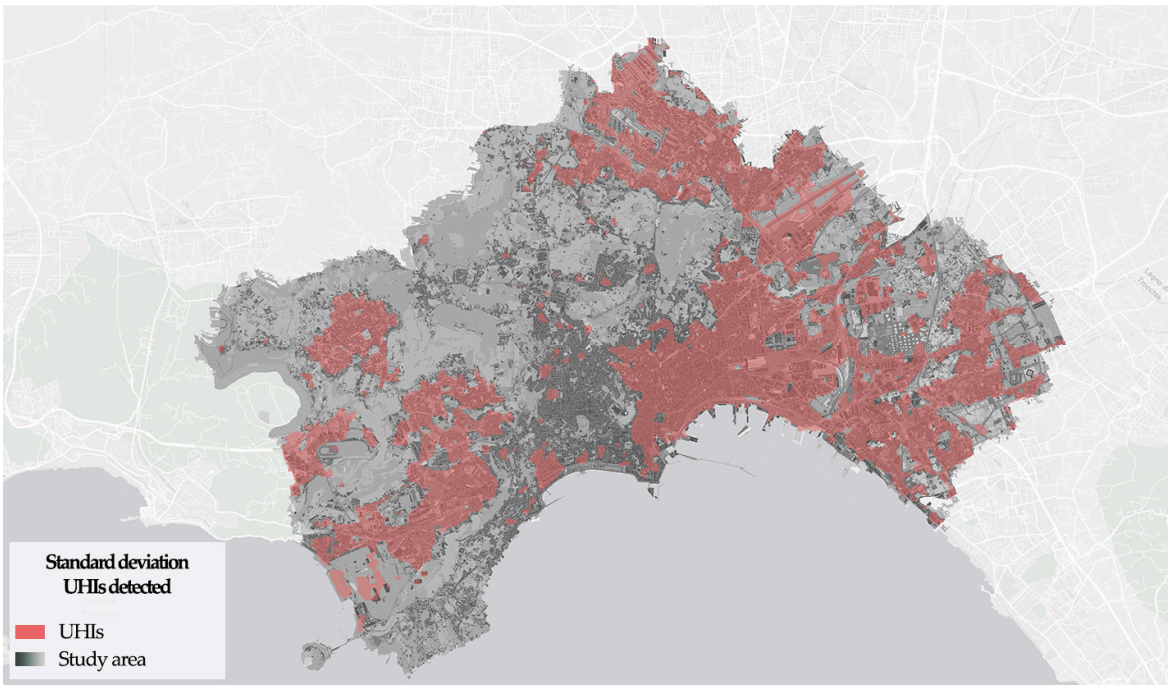

Figure 5. Map of the UHIs detected using the standard deviation method.

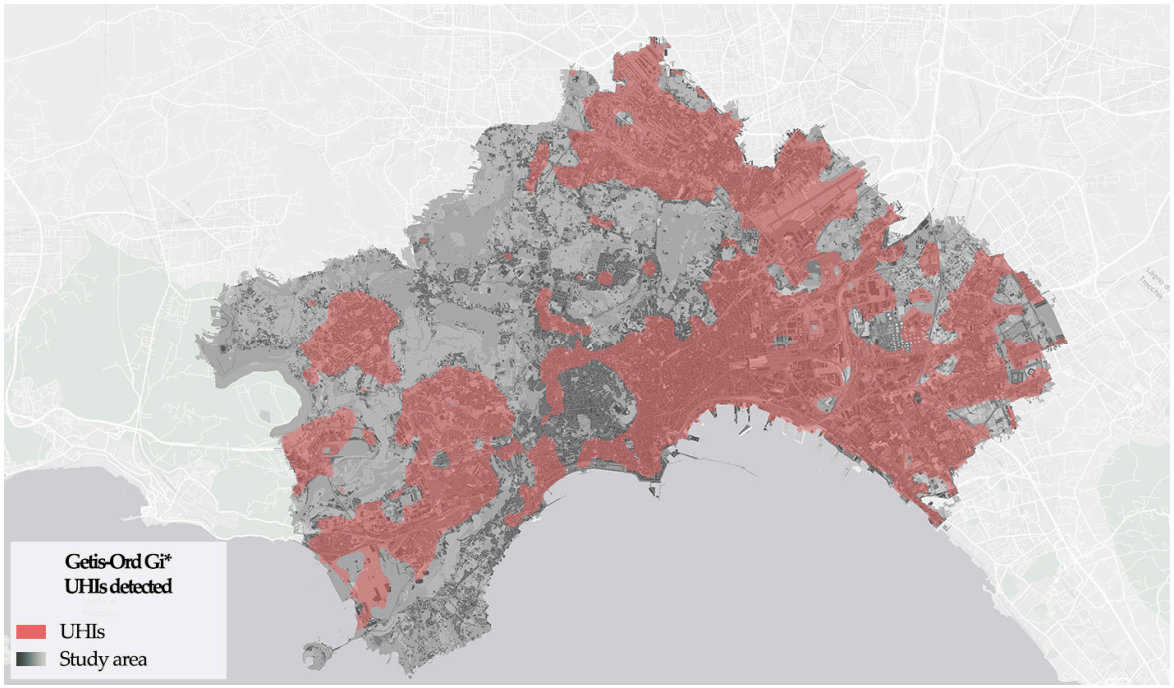

Figure 6. Map of the UHIs detected using Getis-Ord Gi*.

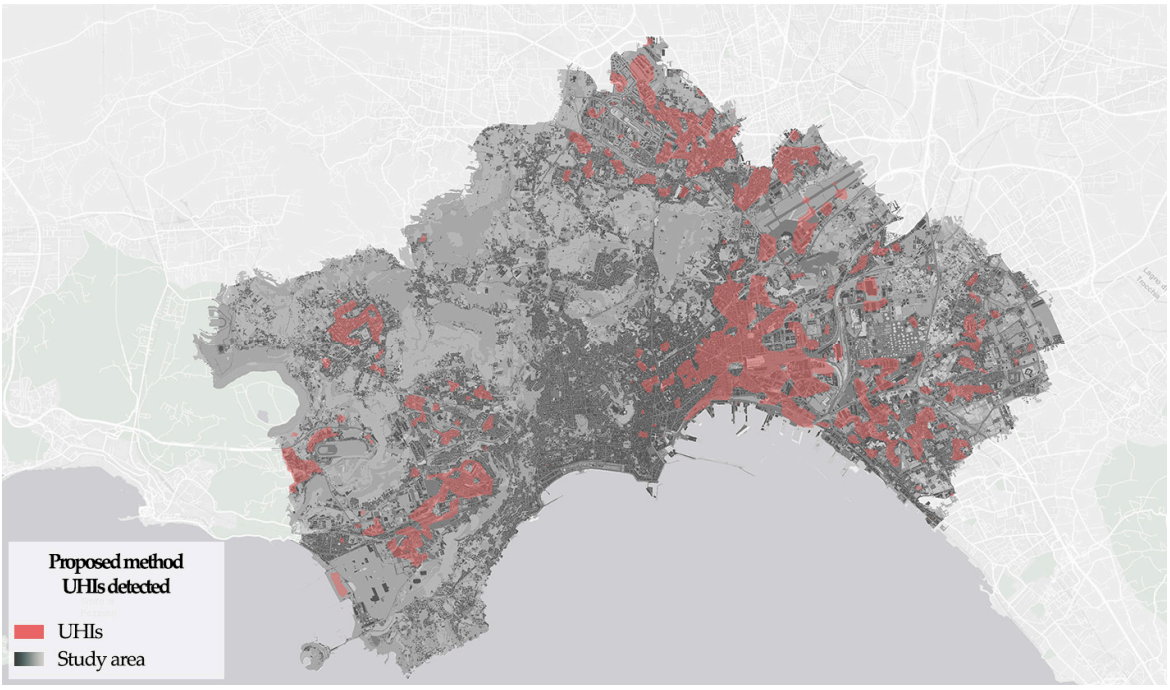

Figure 7. Map of the UHIs detected using the proposed method.

In order to evaluate the effectiveness of the three UHI detection algorithms, we evaluated three characteristics that highlight the typical features of an urban area: the volume of buildings, the permeability of the soil, and the extent of green areas. The measures of these characteristics consist of the following indices (key features):

- Building density, which measures the ratio between the volume of buildings present in the UHI and the overall surface of the UHI;
- Waterproof ratio, which measures the ratio between non-permeable surfaces such as roads, courtyards, car parks, etc., and the entire open space area of the UHI;
- Greenery percentage, which measures the ratio between urban green space surfaces and the overall surface of the UHI.

The values obtained for these three key features in each UHI are compared with those obtained when considering the entire urban settlement and are shown in Table 3.

Table 3. Mean values of the key features obtained for the entire city and for the UHIs detected using the three UHI detection methods.

Key Features	Measured Value in the Urban Settlement	Standard Deviation	Getis-Ord Gi*	Proposed Method
Building density (m^3/m^2)	2.29	11.66	3.06	16.37
Waterproof ratio	0.39	1.09	0.67	1.43
Greenery percentage (%)	23.85%	8.78%	15.70%	3.12%

The results in Table 3 show that, in comparison to the average values of the three key features calculated for the entire city, the method based on the ISODATA algorithm is the best one, as it provides the highest average values of the building density and waterproof ratio (respectively, 16.37 m^3/m^2 and 1.43), and the lowest average value of the greenery percentage (3.12%).

The method that appears to perform the worst is the Getis-Ord GI* method; the values of the key features building density and waterproof ratio (3.06 and 0.67, respectively), although higher than the average values measured over the entire city, are lower than those obtained when performing the other two UHI detection methods. Similarly, the greenery

percentage (15.70%), although lower than the average value measured over the entire city, is lower than the values obtained by performing the other two UHI detection methods.

A more detailed analysis we developed histograms to compare the distribution of each index with the average of the study area.

The histograms in Figures 8–10 show, respectively, the trends in the building density, waterproof ratio, and greenery percentage key features measured in each UHI detected by the three UHI detection methods. The horizontal red line represents the value of the key feature obtained when considering the entire city.

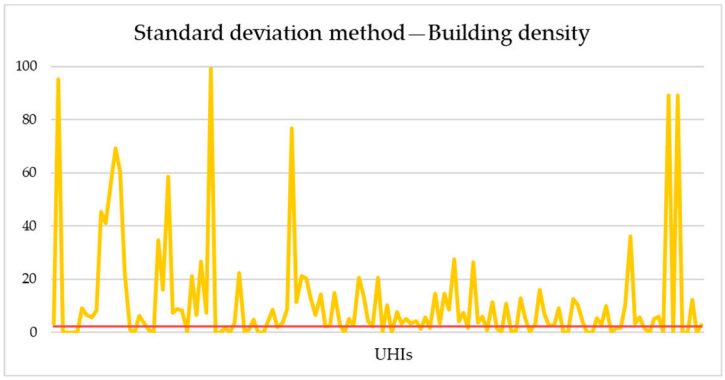

(**a**)

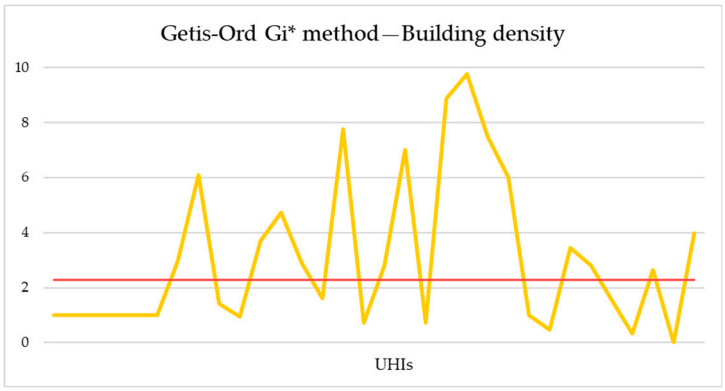

(**b**)

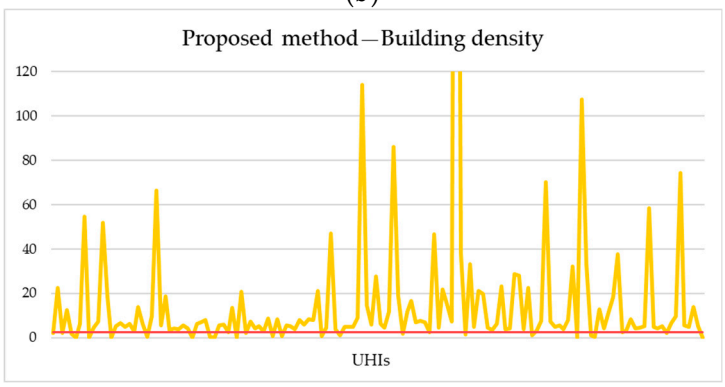

(**c**)

Figure 8. Building density obtained with the standard deviation method (**a**); building density obtained with the Getis-Ord Gi* method (**b**); building density obtained with the proposed method (**c**). The red line represents the value of the building density obtained when considering the entire city.

From the analysis of the three building density trends in Figure 8, it appears that the proposed method is the one in which the UHIs are characterized by a built density much higher than the average built density calculated for the entire city. Over 83% of

the UHIs detected have a built density higher than the city average and over 50% of the UHIs have values higher than three times the city average. The trend observed using the standard deviation method shows a similar behavior, with values of built density higher than the average for about 66% of the UHIs. On the contrary, only in about 50% of the UHIs detected using the Getis-Ord Gi* method is the built density higher than the average for the entire city.

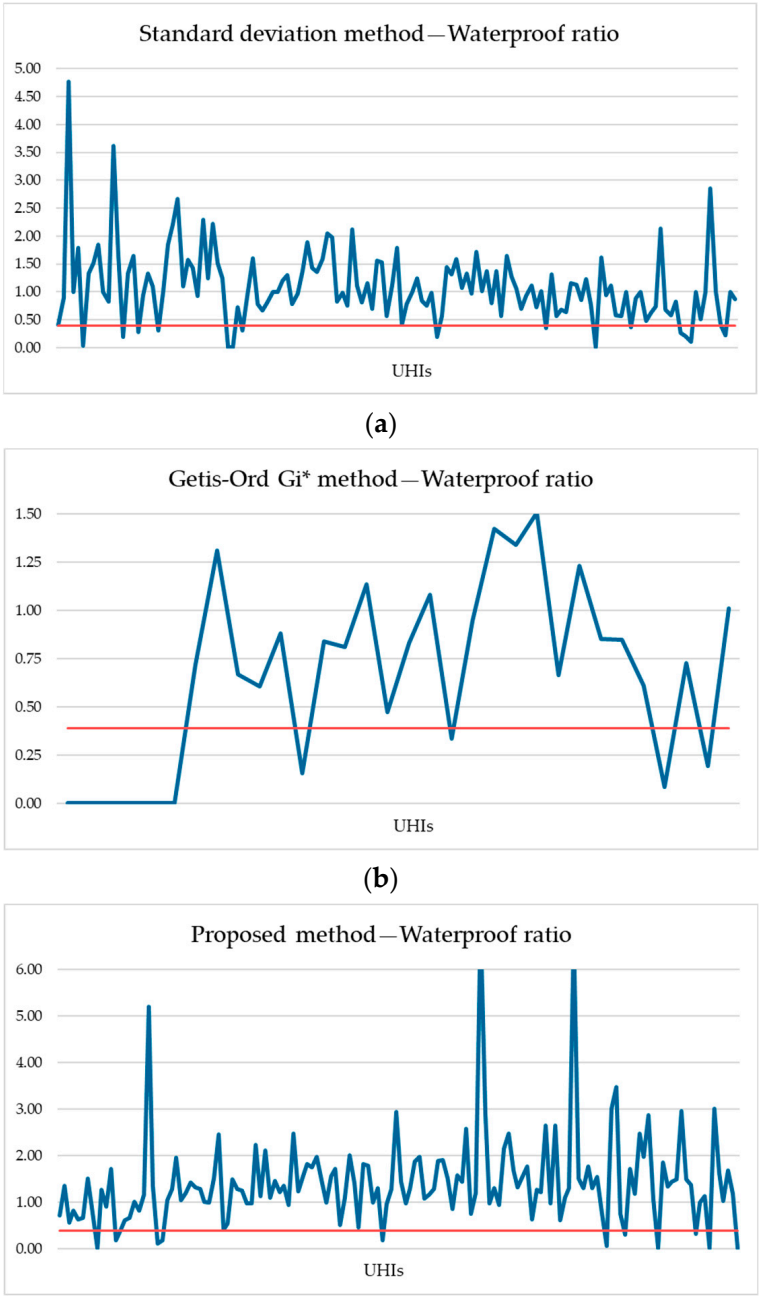

Figure 9. Waterproof ratio obtained with the standard deviation method (**a**); waterproof ratio obtained with the Getis-Ord Gi* method (**b**); waterproof ratio obtained with the proposed method (**c**). The red line represents the value of the waterproof ratio obtained when considering the entire city.

From the trends in Figure 9, it appears that in about 93% of the UHIs detected using our method, the waterproof ratio is higher than the average value calculated for the entire city; furthermore, for over 60% of them, the waterproof ratio is higher than three times this

average value. In over 88% of the UHIs detected using the standard deviation method, the waterproof ratio is higher than the average value calculated for the entire city, while only 69% of the UHIs detected using Getis-Ord Gi* are characterized by waterproof ratio values higher than the average calculated for the entire city.

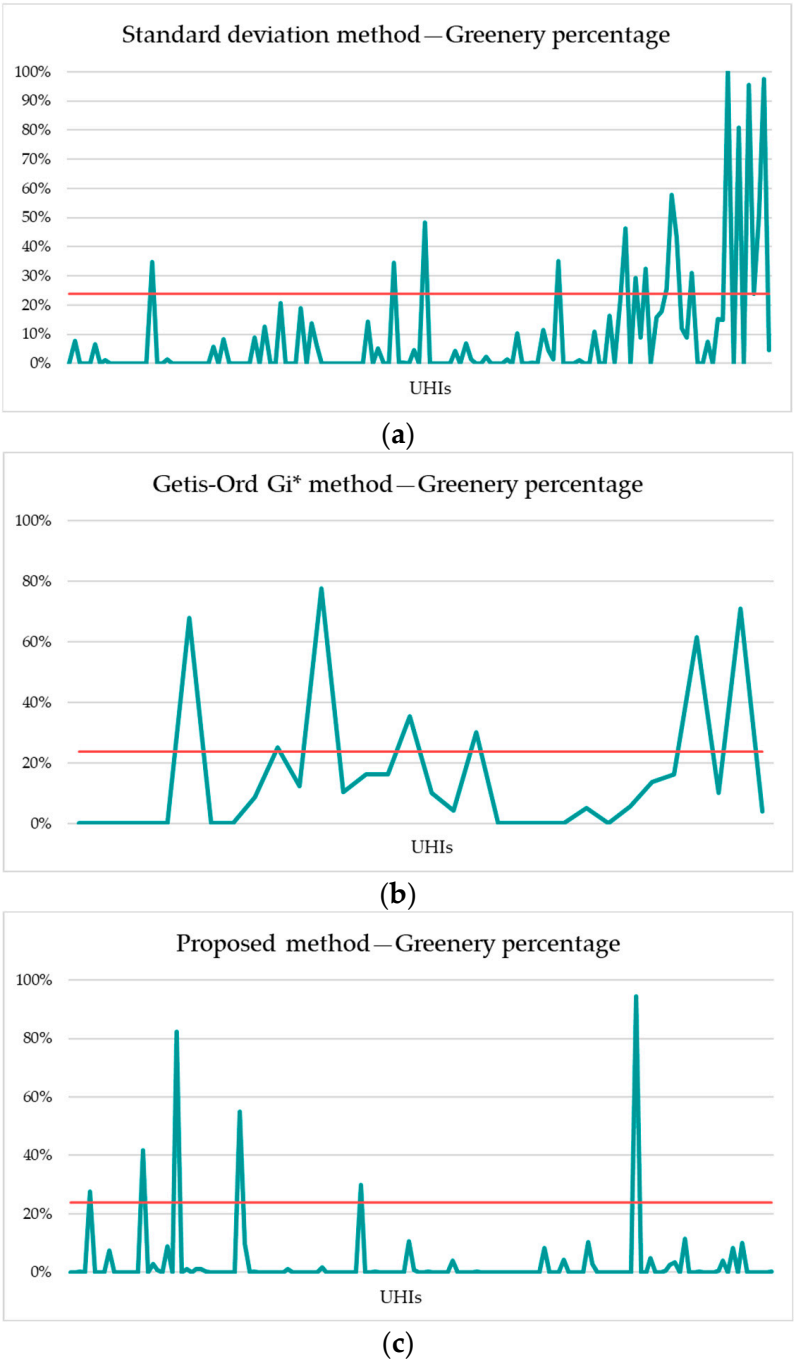

Figure 10. Greenery percentage obtained with the standard deviation method (**a**); greenery percentage obtained with the Getis-Ord Gi* method (**b**); greenery percentage obtained with the proposed method (**c**). The red line represents the value of the greenery percentage obtained when considering the entire city.

The greenery percentage trends in Figure 10 also highlight that the method based on the ISODATA algorithm is the most accurate. In about 96% of the UHIs detected using the proposed method, the greenery percentage is lower than the average calculated for the

entire city, and in over 90% of them the greenery percentage is lower than one third of this average. In almost 87% of the UHIs detected using the standard deviation method, and in about 78% of the UHIs detected using Getis-Ord Gi*, the greenery percentage is lower than the average value calculated for the entire city.

In conclusion, the results obtained relating to the measures of the building density, waterproof ratio, and greenery percentage indices in the UHIs detected using the three methods highlight that the method based on the ISODATA algorithm is the most accurate. It is able to detect UHIs mostly characterized by high building densities and waterproof surfaces, with the rare presence of green surfaces. The method that appears less accurate is Getis-Ord Gi*, which detected a smaller number of UHIs with a greater extension in the city; they are less characterized by high building densities and waterproof surfaces and by a rare presence of green areas.

The results of the comparative tests showed that the proposed method, which optimizes the choice of the parameters for the ISODATA algorithm, such as the number of clusters, the sampling interval, and the minimum class size, provides better accuracy than traditional methods based on standard deviation and Getis-Ord Gi*. It is more robust than the other two UHI detection methods with respect to the presence of noise in the data and determines the shape and size of UHIs with greater accuracy.

4. Conclusions

In this paper, a new unsupervised UHI detection method based on the ISODATA clustering algorithm has been presented. The UHIs are made up of the urban areas belonging to the cluster with the highest average LST.

The proposed UHI detection method has the advantage of determining the optimal cluster number and of being robust to the presence of noise and outliers in the input LST raster image. Furthermore, the method of selecting the data sample from the LST raster dataset allows you to significantly reduce the size of the original raster dataset without incurring data under-sampling.

The main limitation of the method is the low resolution of the LST raster provided by satellite thermal images. A tool that may possibly be useful for increasing the spatial resolution of the LST raster dataset could be thermal cameras mounted on drones; this would require the use of specific resources and expensive data collection campaigns to cover the entire city, and its duration could be longer than that of the heatwave.

The method was implemented on a GIS-based platform and was tested in the city of Naples. The results of the comparative tests against the UHI detection methods Getis-Ord Gi* and standard deviation showed that the proposed method is the most accurate, detecting UHIs with the highest values of building density and waterproof ratio and with the lowest percentage of greenery.

These results highlight that the proposed UHI detection method detects UHIs with a higher accuracy than traditional methods and is, for this reason, more suitable for performing analyses of the location and extent of urban heat islands at detailed urban planning scales.

This framework represents an effective tool for decision makers in the evaluation of the most critical urban areas during heatwaves, when climate-proof actions and strategies to protect the population become a priority.

In the future, we intend to carry out further research to refine the accuracy of this method and carry out experiments with different urban settlements and considering different heatwave scenarios.

Author Contributions: Conceptualization, R.C., B.C., V.D., F.D.M. and V.M.; methodology, R.C., B.C., V.D., F.D.M. and V.M.; software, R.C., B.C., V.D., F.D.M. and V.M.; validation, R.C., B.C., V.D., F.D.M. and V.M.; formal analysis, R.C., B.C., V.D., F.D.M. and V.M.; investigation, R.C., B.C., V.D., F.D.M. and V.M.; resources, R.C., B.C., V.D., F.D.M. and V.M.; data curation, R.C., B.C., V.D., F.D.M. and V.M.; writing—original draft preparation, R.C., B.C., V.D., F.D.M. and V.M.; writing—review and editing, R.C., B.C., V.D., F.D.M. and V.M.; visualization, R.C., B.C., V.D., F.D.M. and V.M.; supervision,

R.C., B.C., V.D., F.D.M. and V.M. All authors have read and agreed to the published version of the manuscript.

Funding: This research received no external funding.

Data Availability Statement: The raw data supporting the conclusions of this article will be made available by the authors on request.

Conflicts of Interest: The authors declare no conflicts of interest.

References

1. Arnfield, A.J. Two Decades of Urban Climate Research: A Review of Turbulence, Exchanges of Energy and Water, and the Urban Heat Island. *Int. J. Climatol.* **2003**, *23*, 1–26. [CrossRef]
2. Barrao, S.; Serrano-Notivoli, R.; Cuadrat, J.M.; Tejedor, E.; Saz Sánchez, M.A. Characterization of the UHI in Zaragoza (Spain) using a quality-controlled hourly sensor-based urban climate network. *Urban Clim.* **2022**, *44*, 101207. [CrossRef]
3. Oke, T.R. City size and the urban heat island. *Atmos. Environ. (1967)* **1973**, *7*, 769–779. [CrossRef]
4. Oke, T.R. The energetic basis of the urban heat island. *Q. J. R. Meteorol. Soc.* **1982**, *108*, 1–24. [CrossRef]
5. IPCC. Climate Change 2022: Impacts, Adaptation and Vulnerability. In *Contribution of Working Group II to the Sixth Assessment Report of the Intergovernmental Panel on Climate Change*; Pörtner, H.-O., Roberts, D.C., Tignor, M., Poloczanska, E.S., Mintenbeck, K., Alegría, A., Craig, M., Langsdorf, S., Löschke, S., Möller, V., et al., Eds.; Cambridge University Press: Cambridge, UK; New York, NY, USA, 2022; p. 3056. [CrossRef]
6. Lacima, A.; Grayson, K.; Chavez, R.; Versteeg, G.; Gonzalez-Reviriego, N.; Doblas-Reyes, F.J.; Soret, A. Heat Waves in Urban Environments—A Destination Earth Use Case in the Climate Adaptation Digital Twin. In Proceedings of the EGU General Assembly 2023, Vienna, Austria, 23–28 April 2023; p. EGU23-10107. [CrossRef]
7. Jusuf, S.K.; Ignatius, M.; Hien, W.N.; Akbari, H. Editorial: Urban Heat Island (UHI) and its Mitigation through Urban Planning, Design, and Landscaping. *Archit. Sci. Rev.* **2018**, *62*, 1–2. [CrossRef]
8. Vardhu, V.A.K.; Sharma, A. Classification, Mitigations and Methods to Detect UHI: A Review. *Indian Sci. J. Res. Eng. Manag.* **2023**, *7*, 26. [CrossRef]
9. Zeynali, R.I.; Bitelli, G.; Mandanici, E. Mobile data acquisition and processing in support of an urban heat island study. *Int. Arch. Photogramm. Remote Sens. Spat. Inf. Sci.* **2023**, *48*, 563–569. [CrossRef]
10. Kimothi, S.; Thapliyal, A.; Gehlot, A.; Aledaily, A.N.; Gupta, A.; Bilandi, N.; Singh, R.; Malik, P.K.; Akram, S.V. Spatio-temporal fluctuations analysis of land surface temperature (LST) using Remote Sensing data (LANDSAT TM5/8) and multifractal technique to characterize the urban heat Islands (UHIs). *Sustain. Energy Technol. Assess.* **2023**, *55*, 102956. [CrossRef]
11. Srashti, S.; Aashutosh, O.; Singh, R.; Kumar, R.; Mehta, A. Analysis of Land Surface Temperature at 10-meter Pixel Size (Spatial Resolution) for Ahmedabad City. In Proceedings of the 2023 International Conference on Computational Intelligence and Sustainable Engineering Solutions (CISES), Greater Noida, India, 28 April 2023; pp. 134–138. [CrossRef]
12. Bruns, J.; Simko, V. Stable Hotspot Analysis for Intra-Urban Heat Islands. *GI_Forum J. Geogr. Inf. Sci.* **2017**, *5*, 70–92. [CrossRef]
13. Lu, Y.; He, T.; Xu, X.; Qiao, Z. Investigation the Robustness of Standard Classification Methods for Defining Urban Heat Islands. *IEEE J. Sel. Top. Appl. Earth Obs. Remote Sens.* **2021**, *14*, 11386–11394. [CrossRef]
14. Chen, S.; Wang, T. Comparison Analyses of Equal Interval Method and Mean-standard Deviation Method Used to Delimitate Urban Heat Island. *Geo-Inf. Sci.* **2009**, *11*, 145–150. [CrossRef]
15. Zhang, J.; Tu, L.; Shi, B. Spatiotemporal Patterns of the Application of Surface Urban Heat Island Intensity Calculation Methods. *Atmosphere* **2023**, *14*, 1580. [CrossRef]
16. Mas'uddin, M.; Karlinasari, L.; Pertiwi, S.; Erizal, E. Urban Heat Island Index Change Detection Based on Land Surface Temperature, Normalized Difference Vegetation Index, and Normalized Difference Built-Up Index: A Case Study. *J. Ecol. Eng.* **2023**, *24*, 91–107. [CrossRef]
17. Li, D.; Wang, L.; Liao, W.; Sun, T.; Katul, G.; Bou-Zeid, E.; Maronga, B. Persistent urban heat. *Sci. Adv.* **2024**, *10*, eadj7398. [CrossRef] [PubMed]
18. Zhang, X.; Kasimu, A.; Liang, H.; Wei, B.; Aizizi, Y.; Zhao, Y.; Reheman, R. Construction of Urban Thermal Environment Network Based on Land Surface Temperature Downscaling and Local Climate Zones. *Remote Sens.* **2023**, *15*, 1129. [CrossRef]
19. Cheng-zeng, Y.; An, S.; Xin-yuan, Y.; Ling, P.; Xiang, L.; Xiao-jing, Y. Observation and forecast on urban heat island effect based on Landsat data. *IOP Conf. Ser. Earth Environ. Sci.* **2017**, *59*, 012043. [CrossRef]
20. Cheval, S.; Dumitrescu, A.; Micu, D.; Onțel, I.; Paraschiv, M.-G.; Simion, G. Heat hazard and risk assessment in urban areas. Case study of Bucharest (Romania). In Proceedings of the EGU General Assembly 2023, Vienna, Austria, 23–28 April 2023; p. EGU23-7133. [CrossRef]
21. Guerri, G.; Crisci, A.; Messeri, A.; Congedo, L.; Munafò, M.; Morabito, M. Thermal Summer Diurnal Hot-Spot Analysis: The Role of Local Urban Features Layers. *Remote Sens.* **2021**, *13*, 538. [CrossRef]
22. Orusa, T.; Borgogno Mondino, E. Landsat 8 thermal data to support urban management and planning in the climate change era: A case study in Torino area, NW Italy. In Proceedings of the Remote Sensing Technologies and Applications in Urban Environments IV, Strasbourg, France, 9–10 September 2019; Volume 11157, pp. 1–17. [CrossRef]

23. Luo, Y.; Jiang, Y.; Khan, S.; Peng, S.; Feng, Y.; Han, B. Analysis of urban heat island effect using k-means clustering. In Proceedings of the 2nd International Conference on Information Science and Engineering, Hangzhou, China, 4–6 December 2010; pp. 3543–3546. [CrossRef]
24. Chen, X.; Zongmin, W.; Haibo, Y.; Alistair, C.F.; Richard, J.D. Impacts of urban densification and vertical growth on urban heat environment: A case study in the 4th Ring Road area, Zhengzhou, China. *J. Clean. Prod.* **2023**, *410*, 137247. [CrossRef]
25. Cardone, B.; Di Martino, F.; Miraglia, V. A Novel Fuzzy-Based Remote Sensing Image Segmentation Method. *Sensors* **2023**, *23*, 9641. [CrossRef]
26. Ahmad, A.; Sufahani, S.F. Analysis of Landsat 5 TM data of Malaysian land covers using ISODATA clustering technique. In Proceedings of the 2012 IEEE Asia-Pacific Conference on Applied Electromagnetics (APACE), Melaka, Malaysia, 11–13 December 2012; pp. 92–97. [CrossRef]
27. Youme, S.K.; Abid, M.S.; Chowdhury, T.A.; Ahamed, H.; Siddique, S. Local Climate Zone Mapping Using Clustering Algorithms: A Case Study of Dhaka, Bangladesh. In Proceedings of the IGARSS 2022—2022 IEEE International Geoscience and Remote Sensing Symposium, Kuala Lumpur, Malaysia, 17–22 July 2022; pp. 3139–3142. [CrossRef]
28. Zhao, Y.; Zhong, Z.; Zhou, K.; Liu, B.; Shu, W. Responses of the Urban Atmospheric Thermal Environment to Two Distinct Heat Waves and Their Changes with Future Urban Expansion in a Chinese Megacity. *Geophys. Res. Lett.* **2024**, *51*, e2024GL109018. [CrossRef]
29. Guo, Y.; Shao, C.; Su, A. Investigation of Land–Atmosphere Coupling during the Extreme Rainstorm of 20 July 2021 over Central East China. *Atmosphere* **2023**, *14*, 1474. [CrossRef]
30. Jiang, X.; Zhang, D.; Luo, Y. Influences of Urbanization on an Afternoon Heavy Rainfall Event over the Yangtze River Delta Region. *Montly Weather. Rev.* **2023**, *151*, 815–832. [CrossRef]